02 Jun 1993, 9:00 am - 12:00 pm

Testing of Drilled Shafts Socketed Into Limestone

G. L. Panozzo
CH2M HILL, Tampa, Florida

F. H. Kulhawy
Cornell University, Ithaca, New York

F. C. Bauhof
CH2M HILL, Tampa, Florida

A. J. O'Brien
CH2M HILL, Tampa, Florida

Proceedings: Third International Conference on Case Histories in Geotechnical Engineering, St. Louis, Missouri, June 1-4, 1993, Paper No. 1.47

Testing of Drilled Shafts Socketed Into Limestone

G. L. Panozzo
CH2M HILL, Tampa, Florida

F. C. Bauhof
CH2M HILL, Tampa, Florida

F.H. Kulhawy
Cornell University, Ithaca, New York

A. J. O'Brien
CH2M HILL, Tampa, Florida

SYNOPSIS: Construction of the first phase of the South Parking Garage at the Tampa International Airport in Florida was completed in December 1991. A full-scale field load testing program was used in design of the drilled shaft foundations, with specific goals of determining the bond strength and characterizing the load-displacement behavior of the rock sockets.

The displacement behavior and bond strength of the test shafts were predicted from elastic solutions and semi-empirical methods. Input parameters included the rock uniaxial compressive strength and elastic modulus. The load test results are compared to the predictions herein, and the practical application of these comparisons is demonstrated by a sample evaluation of a drilled shaft supporting the South Parking Garage.

INTRODUCTION

Drilled shaft foundations must satisfy the same design criteria as other types of foundation systems: adequate stability, tolerable deformations, and cost-effectiveness. This paper presents a comparative study of the field-monitored and analytically-predicted behavior of drilled shafts socketed into rock and subjected to compressive axial loads. The results of this comparative study are used to evaluate the performance of drilled shafts through a design example.

The load test program was conducted as part of the geotechnical design for the South Parking Garage at the Tampa International Airport in Tampa, Florida. The building footprint is in excess of 4.5 hectares (11 acres), with over 300 columns supporting typical axial loads of 9.5 MN (2,130 kip). A single drilled shaft socketed into the underlying weathered limestone provides support for the columns.

SITE CHARACTERIZATION

The overburden soils at the load test site are part of the Gulf Coastal Lowlands physiographic province. Undifferentiated deposits of Pleistocene and Recent age form the overburden within this province (White, 1970). The overburden soils are underlain by sedimentary rocks to depths of greater than 3,000 m (10,000 ft). The surface of the bedrock is the Tampa Limestone of Miocene age (Menke, Meredith, and Wetterhall, 1961).

The limestone at the load test site is overlain by 4.6 m (15 ft) of soil overburden, and the groundwater is at a depth of 2.4 m (8 ft). Extensive weathering has resulted in solutioning of the limestone, leading to numerous soil-filled voids. The limestone was characterized by 10 uniaxial compression tests on intact cores recovered from the load test site. These cores had an average uniaxial compressive strength of 4.67 MPa (97.5 ksf) and an average elastic modulus of 1.99 GPa (41,500 ksf). The average rock quality designation (RQD) of all limestone cores at the load test site was 55 percent.

LOAD TEST PROGRAM

The load test program consisted of 8.9 MN (2,000 kip) static tests on two drilled shafts, designated Test Shaft 1 and 2. The test shafts were installed using wet hole construction techniques. A biopolymer drilling fluid additive and a permanent steel casing were used to stabilize the shaft excavations within the overburden soils. The rock sockets were excavated with auger bits, and a clean-out bucket was used to remove sidewall slough and drill cuttings. Instrumented reinforcing steel cages were lowered into the shaft excavations, and a high slump concrete was placed by tremie methods.

The geometries of the test shafts are shown in Fig. 1. Test Shaft 1 was constructed with a false bottom to eliminate shaft tip resistance. The drilled shafts were instrumented with vibrating wire strain gages and telltales at the locations shown in Fig. 1. Displacements of the telltales, as well as the test shaft

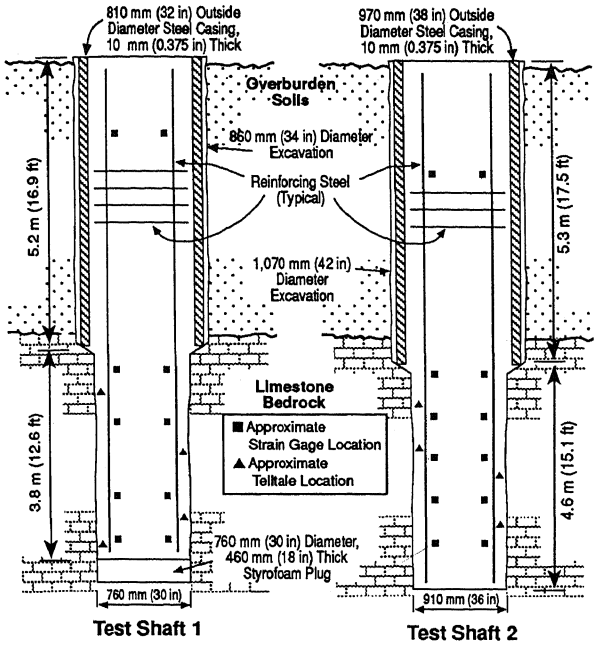

Fig. 1. Geometries of Test Shafts

butts, were measured with dial gages. The load to the test shafts was applied with a hydraulic jack and measured with a calibrated load cell. Test Shaft 1 was tested with one load/unload cycle. Test Shaft 2 was tested with two/unload cycles. The first cycle was up to 3.6 MN (800 kip), and the second was up to the total test load of 8.9 MN (2,000 kip). Data from the load test instrumentation were recorded at nominal 2, 6, and 10-minute increments following each level of load application.

EXPECTED TEST SHAFT RESPONSE

When a drilled shaft is loaded in axial compression, the applied load generally is supported in side resistance along the drilled shaft socket and in tip resistance at the bottom of the shaft socket. The distribution of the load between side and tip resistance is a function of the drilled shaft geometry, the relative stiffnesses of the drilled shaft and rock mass, and the displacement of the shaft butt. When relatively low levels of load are applied, the drilled shaft responds in essentially a linear manner. Elastic theory can be used to characterize the load transfer and load-displacement response, as illustrated in Fig. 2 by the line OA.

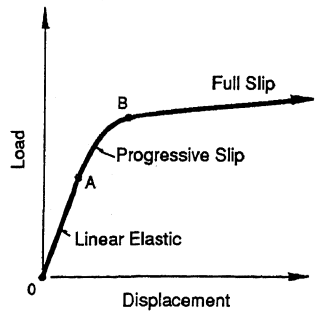

Fig. 2. Idealized Drilled Shaft Load-Displacement Response

As the load is increased beyond point A in Fig. 2, the shear stress at some locations along the shaft sides will exceed the concrete-rock bond strength, resulting in relative displacement between the shaft and surrounding rock. If loading is continued beyond point B in Fig. 2, the concrete-rock bond strength along the entire circumference of the rock socket will be exceeded, and relative displacement will result between the shaft and surrounding rock along the entire interface .

Linear Elastic Response

The theory of elasticity can be used to characterize the drilled shaft load-displacement response at low load levels that result only in shear transfer and no bond failure along the shaft sides. The drilled shaft is assumed to be a cylindrical elastic inclusion within a surrounding rock and soil mass as shown in Fig. 3. An axial compressive load (Q_c) at the shaft butt of either a complete socket or a shear socket is assumed. Test Shaft 1 modeled a shear socket, and Test Shaft 2 modeled a complete socket. The drilled shaft is characterized by the diameter (B), depth within the soil overburden (D_s), depth of rock socket (D_r), elastic modulus (E_c), and Poisson's ratio (ν_c). The rock is characterized above the shaft tip by a rock mass elastic modulus (E_r) and Poisson's ratio (ν_r) and below the shaft tip by a rock mass elastic modulus (E_b) and Poisson's ratio (ν_b).

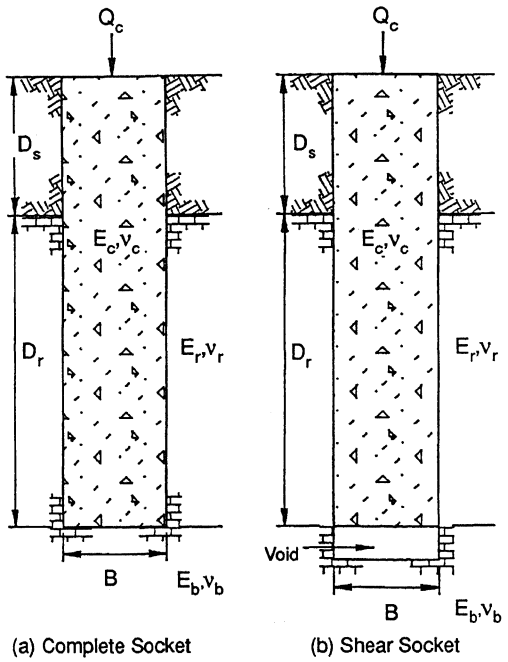

Fig. 3. Compression Loading of Drilled Shaft

The linear elastic load-displacement response of a shear socket, or simply the ratio of the compression

load applied to the shaft at the top of the rock socket (Q_r) to the displacement of the shaft at the top of the rock socket (w_r), can be approximated from elastic theory by (Carter and Kulhawy, 1988):

$$\frac{Q_r}{w_r} = E_r \left[\frac{\pi D_r}{(1+\nu_r) \ln [5(1-\nu_r) D_r/B]} \right] \quad (1)$$

Essentially all of the load applied to the butt of the test shafts is expected to be transmitted to the rock socket portion of the shafts. Therefore, the load applied to the shaft butt (Q_c) can be assumed to be equal to Q_r in Eq. 1.

The linear elastic load-displacement response of a complete socket can be approximated from elastic theory by (Carter and Kulhawy, 1988):

$$\left[\frac{Q_r}{w_r} - \frac{Q_{tip}}{w_r} \right] = E_r \left[\frac{\pi D_r}{(1+\nu_r) \ln [5(1-\nu_r) D_r/B]} \right] \quad (2)$$

and

$$\frac{Q_{tip}}{w_r} = E_b \left[\frac{B}{1-\nu_b^2} \right] \quad (3)$$

The variable Q_{tip} in Eqs. 2 and 3 is the load transmitted to the tip of the rock socket.

The rock property parameters in Eqs. 1 through 3 include the rock mass modulus and Poisson's ratio. Variations in Poisson's ratio for most rock materials is limited and can be approximated as 0.25. Estimates can be made of the rock mass modulus in MPa as a function of the rock uniaxial compressive strength (q_u) in MPa (Rowe and Armitage, 1986) by:

$$E_r \text{ or } E_b = 215 \sqrt{q_u} \quad (4)$$

For the average uniaxial compressive strength of the rock at the load test site of 4.67 MPa (97.5 ksf), Eq. 4 results in an estimated rock mass modulus of 465 MPa (9,710 ksf). Alternatively, the rock mass modulus can be estimated as a function of the elastic modulus of intact cores (E_i) by (Kulhawy and Goodman, 1980):

$$E_r \text{ or } E_b = \alpha_E E_i \quad (5)$$

in which α_E is a modulus reduction factor. The modulus reduction factor can be estimated from the RQD of the rock and the ratio of rock mass modulus to the normal stiffness of discontinuities. Using the average RQD of cores from the load test site, which equals 55 percent, and 1 m (3.28 ft) for the rock modulus to discontinuity stiffness ratio, which is reported as the mean of typical ranges in hard, non-porous rock, α_E is expected to be approximately 10 percent (Kulhawy and Goodman, 1980). This value of α_E can be substituted into Eq. 5 with the average elastic modulus of intact cores at the load test site to estimate a rock mass modulus of 199 MPa (4,150 ksf).

The expected linear elastic load-displacement response of Test Shaft 1 can be predicted by substituting the rock parameters described above and the test shaft geometries into Eq. 1. This results in a predicted response or Q_r/w_r ratio equal to 1.53 MN/mm (8,730 kip/in) for a rock modulus determined from the uniaxial compressive strength and 0.66 MN/mm (3,770 kip/in) using the estimated modulus reduction factor. The expected linear response of Test Shaft 2 can be predicted similarly using Eqs. 2 and 3. The results are summarized in Table 1.

Table 1. Predicted Load-Displacement of Test Shaft 2

	Q_r/w_r MN/mm (kip/in)	Q_{tip}/w_r MN/mm (kip/in)
Rock mass modulus determined from uniaxial compressive strength	2.28 (13,000)	0.45 (2,570)
Rock mass modulus determined from estimated reduction factor	0.97 (5,540)	0.19 (1,080)

Concrete-Rock Bond Strength

Available methods to evaluate the average concrete-rock bond strength along drilled shafts (τ_{max}) are based primarily on semi-empirical factors and the rock uniaxial compressive strength. These methods are summarized in Table 2, along with the anticipated response of the test shafts for the average uniaxial compressive strength at the load test site of 4.67 MPa (97.5 ksf). All of the load applied to Test Shaft 1 will be transmitted to the concrete-rock bond because the

Table 2. Concrete-Rock Bond Strength Predicted by Various Methods

Method	Average Concrete-Rock Bond Strength, τ_{max} MPa (ksf)	Predicted Test Shaft 1 Concrete-Rock Bond Capacity MN (kip)	Predicted Test Shaft 2 Concrete-Rock Bond Capacity MN (kip)
$\frac{\tau_{max}}{p_a} = 0.63 \text{ to } 0.95 \sqrt{\frac{q_u}{p_a}}$ (Carter & Kulhawy, 1988)[a]	0.43 to 0.65 (9.0 to 13.6)	3.96 to 5.98 (889 to 1,340)	5.68 to 8.59 (1,280 to 1,930)
$\tau_{max} = 0.45 \text{ to } 0.60 \sqrt{q_u}$ (Rowe & Armitage, 1987)[b]	0.97 to 1.30 (20.3 to 27.1)	8.92 to 11.6 (2,000 to 2,610)	12.8 to 17.2 (2,880 to 3,870)
$\tau_{max} = 0.2\, q_u$ (Pells, Rowe & Turner, 1980)[c]	0.93 (19.4)	8.56 (1,920)	12.3 (2,760)

[a] p_a is atmospheric pressure
[b] q_u in MPa
[c] Applicable for rough sockets

shaft was constructed as a shear socket. Therefore, the method estimating τ_{max} by Carter and Kulhawy predicts that the concrete-rock bond strength at Test Shaft 1 will be exceeded before the total planned load of 8.9 MN (2,000 kip) is applied. However, the other methods shown in Table 2 predict a strength of the concrete-rock bond that is approximately equal to or greater than the anticipated applied load.

The load applied to Test Shaft 2 will be transmitted to the concrete-rock bond and shaft tip because the shaft was constructed as a complete socket. Eqs. 2 and 3 can be combined to predict a ratio of load in the shaft tip to load in the concrete-rock bond of 19 percent for a ratio of rock mass modulus along the shaft side to that at the shaft base equal to 1.0. Therefore, up to 7.2 MN (1,620 kips) of the total planned test load is expected to be transmitted to the shaft concrete-rock bond. This amount falls within the range of concrete-rock bond capacity determined by the Carter and Kulhawy method and is less than the amount in the other methods.

LOAD TEST RESULTS

Test Shaft 1

The average butt displacements at the 10-minute increment during testing of Shaft 1 are shown in Fig. 4. An average displacement of approximately 97 mm (3.80 in) was measured for the maximum applied load of 8.9 MN (2,000 kip). The strain gage data were used to determine the load in the shaft. The modulus of elasticity of the test shafts (E_c) was determined for each level of applied load based on the data from the pair of strain gages directly below the shaft butt. The load calculated at the location of the strain gages using this modulus is shown in Fig. 5 for Test Shaft 1. Decreases in load with depth in the shaft indicate that load is being transferred to the rock surrounding the shaft. The load distribution curves show that essentially all of the applied load is transferred to the rock socket. In addition, the data demonstrate that the false bottom placed at the shaft tip eliminated essentially all tip loading.

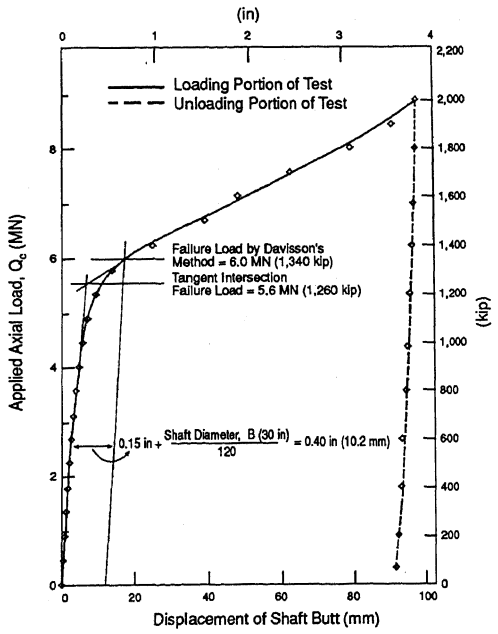

Fig. 4. Average Butt Displacements in Test Shaft I

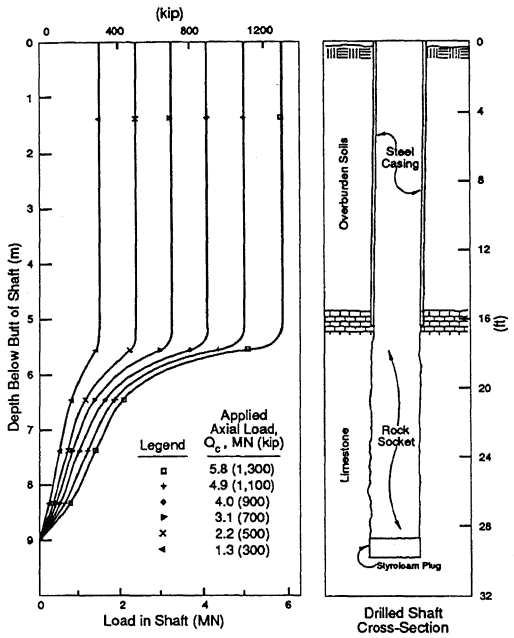

Fig. 5. Load Distribution in Test Shaft I

Test Shaft 2

The average butt displacements at the 10-minute increment during testing of Shaft 2 are shown in Fig. 6.

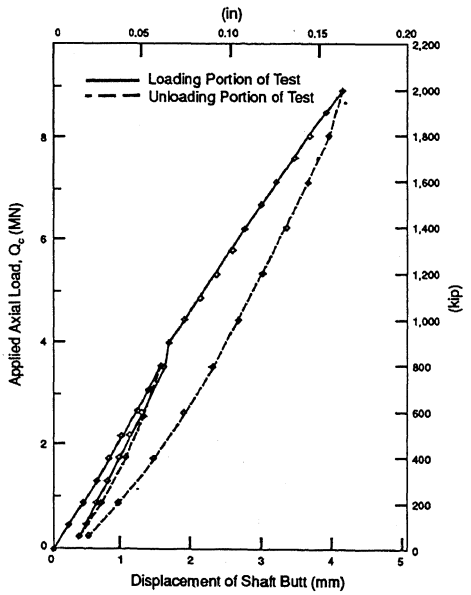

Fig. 6. Average Butt Displacements in Test Shaft 2

An average displacement of approximately 4 mm (0.16 in) was measured for the maximum applied load of approximately 8.9 MN (2,000 kip). The strain gage data were used to determine the load in the shaft as described for Test Shaft 1, and the results are shown in Fig. 7. Again, the load distribution curves show that essentially all of the applied load was transferred to the rock socket. The load distribution data at the strain gage locations were extrapolated as shown to the tip of the rock socket to estimate the tip load.

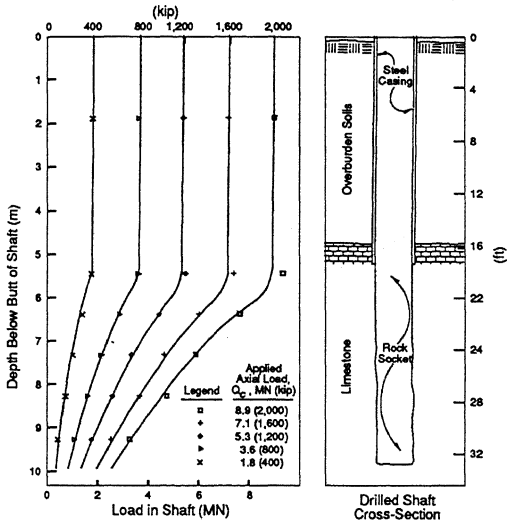

Fig. 7. Load Distribution in Test Shaft 2

COMPARISONS WITH PREDICTED RESPONSES

Test Shaft 1

The linear elastic load-displacement response of Test Shaft 1, or simply the ratio of the compression load at the top of the rock socket (Q_r) to the displacement of the shaft at the top of the rock socket (w_r), is shown in Fig. 8. The Q_r value in Fig. 8 is equal to that applied to the test shaft butt, because no significant load transfer occurred in the soil overburden. The displacements shown were determined by subtracting the relative displacement of the shaft butt and shaft at the top of the rock socket (w_{cr}), given by the following equation, from the observed shaft butt displacements shown in Fig. 4:

$$w_{cr} = \frac{4Q_c D_s}{\pi B^2 E_c} \qquad (6)$$

The initial linear slope of the test data in Fig. 8 is equal to approximately 1.95 MN/mm (11,100 kip/in). Also shown in Fig. 8 are the linear elastic responses previously predicted for Test Shaft 1. The actual slope was approximately 1.3 times greater than that predicted using the uniaxial compressive strength and 3.0 times greater than that predicted using an estimated modulus reduction factor of 10 percent.

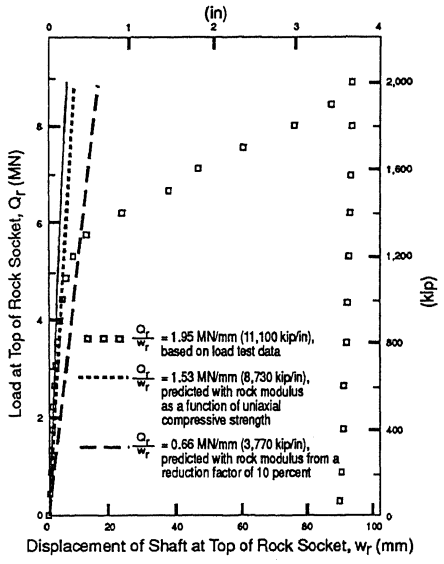

Fig. 8. Load-Displacement Behavior of Test Shaft 1

The rate of shaft butt displacement in Fig. 4 increased at applied loads between approximately 5 and 6 MN (1,100 and 1,300 kip). The tangent intersection method can be used to interpret the failure load by drawing two tangents to the load-displacement data, as shown in Figure 4. This procedure gives an interpreted failure load of 5.6 MN (1,260 kip). Davisson's method also can be used to interpret a failure load (Davisson, 1972). This method consists of drawing a line parallel to the initial straight line tangent of the load-displacement data. Then a parallel line is drawn to intersect the displacement axis at a displacement of 0.15 in (3.8 mm), plus the shaft diameter in inches divided by 120, as shown in Figure 4. The intersection of the parallel line and the test data gives an interpreted failure load of 6.0 MN (1,340 kip). The actual capacity of the rock socket was within the range of predicted values in Table 2 for the Carter and Kulhawy method, but it was less than the values for the other referenced methods.

Test Shaft 2

The load applied to the top of the Test Shaft 2 rock socket (Q_r) and the associated displacement of the top of the rock socket (w_r) are shown in Fig. 9. The loads and displacements in Fig. 9 were determined in the same manner as described above for Test Shaft 1. The slope of this load-displacement data is approximately 2.3 MN/mm (13,100 kip/in). Also shown in Fig. 9 are the predicted load-displacement responses. The actual slope of the test data is approximately the same as that predicted using the uniaxial compressive strength, but it is approximately 2.4 times greater than predicted when using a modulus reduction factor of 10 percent.

The load transmitted to the tip of the socket (Q_{tip}), determined as described previously, and the predicted responses also are shown in Fig. 9. The slope of the tip load-displacement data is approximately 0.55

MN/mm (3,140 kip/in), which is approximately 1.2 times greater than that from the uniaxial compressive strength and 2.9 times that from a modulus reduction factor of 10 percent.

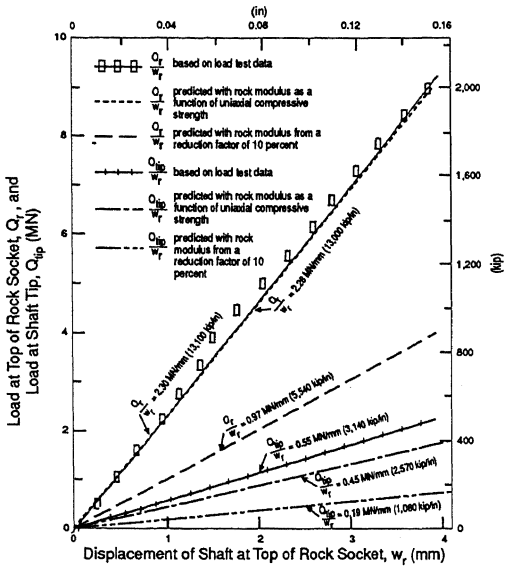

Fig. 9. Load-Displacement Behavior of Test Shaft 2

Fig. 10 shows the variation in the amount of load transferred to the tip in Test Shaft 2. Also shown is the predicted tip load, which is 19 percent of that applied to the shaft butt. The predicted load correlates well with the actual load transmitted.

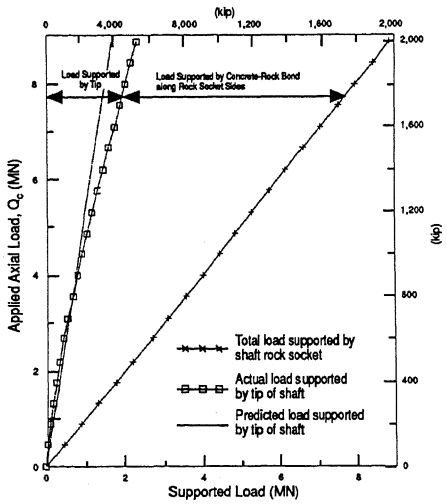

Fig. 10. Relative Load Transfer in Test Shaft 2

As shown in Fig. 6, the rate of butt displacement did not increase with applied load in Test Shaft 2, and therefore the concrete-rock bond strength of the socket was not exceeded. The maximum load applied to the rock socket sides was approximately 6.6 MN (1,400 kip), considering the actual amount transmitted to the tip and the maximum applied butt load of 8.9 MN (2,000 kip). This side load is within the range predicted in Table 2 by the Carter and Kulhawy method, but it is less than that predicted from the other referenced methods.

CONCLUSIONS AND PRACTICAL APPLICATIONS

In general, the displacements of the test shafts were less than anticipated, because the rock mass modulus was underestimated. The displacements of the load test drilled shafts were predicted using elastic theory with a rock mass modulus determined as a function of uniaxial compressive strength and using a modulus reduction factor of 10 percent. However, the load test results can be used to determine the appropriate rock mass modulus at the test site. Substituting the slope of the data for Test Shaft 1 in Fig. 8 into Eq. 1 and for Test Shaft 2 in Fig. 9 into Eqs. 2 and 3 results in the rock mass moduli summarized in Table 3. Also shown in Table 3 are modulus reduction factors that are based on the load test results and the average elastic modulus of intact cores at the load test site, which equals 1.99 GPa (41,500 ksf). These α_E values are larger than the average values for hard, non-porous rock. The rock at this site is both soft and porous, indicating less modulus reduction as a result of jointing.

Table 3. Rock Mass Moduli Determined From Load Test

Description	Rock Mass Modulus, E_r or E_b MPa (ksf)	Modulus Reduction Factor, α_E = E_r or E_b/E_i (percent)
Above Test Shaft 1 Tip	590 (12,400)	30
Above Test Shaft 2 Tip	440 (9,200)	22
Below Test Shaft 2 Tip	560 (11,800)	29

The elastic modulus of over 300 intact rock cores from across the planned South Parking Garage site was determined. The average within the anticipated depths of the planned drilled shaft rock sockets for foundation support of the structure is 690 MPa (14,400 ksf). The modulus reduction factors determined from the load test were used to estimate a rock mass modulus ranging from 150 to 210 MPa (3,170 to 4,320 ksf) surrounding the sockets being considered. The estimated rock mass modulus for the site can be substituted into Eqs. 2 and 3, with socket geometries, axial load, and an assumed Poisson's ratio of 0.25 for the rock mass. This results in an estimated displacement range of 6 to 8 mm (0.24 to 0.32 in) at the top of a rock socket with a diameter of 1.22 m (4.0 ft), length of 8.2 m (27 ft), and axial load of 9.5 MN (2,130 kip). The butt displacement can be estimated by adding the displacement at the top of the rock socket to the relative displacement between the shaft butt and top of the rock socket. This relative displacement can be conservatively estimated using Eq. 6, which assumes that no load is transmitted to the.

overburden soils within the top portion of the shafts. Substituting the appropriate parameters described above into Eq. 6, assuming an average thickness of overburden soils of 4.6 m (15 ft) and an elastic modulus of 21,000 MPa (430,000 ksf) for the drilled shafts, gives a relative displacement of approximately 2 mm (0.08 in.). Therefore, a total butt displacement less than 10 mm (0.4 in) is anticipated for the drilled shafts providing support for the 9.5 MN (2,130 kip) column loads.

The concrete-rock bond strength of the load test drilled shafts was estimated using several methods based on semi-empirical factors and functions of the rock uniaxial compressive strength. The method that predicted the load test results most closely was that given by Carter and Kulhawy (1988):

$$\frac{\tau_{max}}{p_a} = 0.63 \text{ to } 0.95 \sqrt{\frac{q_u}{p_a}} \qquad (7)$$

The semi-empirical factor in this method ranges from 0.63 to 0.95, but the load test results can be used to determine an appropriate design factor for this site. The site design factor can be calculated using an actual capacity of approximately 5.8 MN (1,300 kips) for Test Shaft 1 and an average uniaxial compressive strength of 4.66 MPa (97.5 ksf) for rock cores from the load test site. This procedure results in a semi-empirical factor of 0.92 that can be used to evaluate the rock sockets in the area of the load test as follows:

$$\frac{\tau_{max}}{p_a} = 0.92 \sqrt{\frac{q_u}{p_a}} \qquad (8)$$

The uniaxial compressive strength of over 300 rock cores from across the planned site of the South Parking Garage was determined, and the average within the planned depth of the rock sockets is 2.6 MPa (53.3 ksf). The average uniaxial compressive strength can be substituted into Eq. 8 to determine the concrete-rock bond capacity of the rock sockets under consideration. This results in a concrete-rock bond capacity of 14.8 MN (3,330 kip) for a rock socket with a diameter of 1.22 m (4.0 ft) and length of 8.2 m (27 ft).

ACKNOWLEDGMENTS

The authors wish to thank the Hillsborough County Aviation Authority for its support in the load test program and authorization to discuss the results.

REFERENCES

Carter, J. P. and Kulhawy, F. H. (1988). "Analysis and Design of Drilled Shaft Foundations Socketed into Rock." *Report EL-5918*, Electric Power Research Institute, Palo Alto, 188 p.

Davisson, M. T., (1972) "High Capacity Piles." *Proceedings*, Lecture Series on Innovations in Foundation Construction, ASCE Illinois Section, Chicago, 52 p.

Kulhawy, F. H. and Goodman, R. E. (1980). "Design of Foundations on Discontinuous Rock." *Proceedings*, International Conference on Structural Foundations on Rock, Vol. 1, Sydney, pp. 209-220.

Menke, C. G., Meredith, E. W., and Wetterhall, W. S. (1961). "Water Resources of Hillsborough County, Florida." *Report of Investigations No. 25*, State of Florida States Board of Conservation, Florida Geological Survey, Tallahassee, 100 p.

Pells, P.J.N., Rowe, R.K., and Turner, R.M. (1980). "An Experimental Investigation into Side Shear for Socketed Piles in Sandstone." *Proceedings*, International Conference on Structural Foundations on Rock, Vol. 1, Sydney, pp. 291-302.

Rowe, R.K. and Armitage, H.H., (1986). "A Design Method for Drilled Piers in Soft Rock." Canadian Geotechnical Journal, Vol. 24, pp. 126-142.

White, W. A. (1970). "The Geomorphology of the Florida Peninsula." *Geological Bulletin No. 51*, State of Florida Department of Natural Resources, Bureau of Geology, Tallahassee, 164 p.

NOTATION

The following symbols are used in this paper:

B	=	diameter of drilled shaft
D_r	=	length of drilled shaft socketed into rock
D_s	=	length of drilled shaft in soil overburden
E_b	=	rock mass elastic modulus below the drilled shaft tip
E_c	=	elastic modulus of drilled shaft
E_i	=	elastic modulus of intact rock core
E_r	=	rock mass elastic modulus above the drilled shaft tip
p_a	=	atmospheric pressure
Q_c	=	axial compressive load applied to drilled shaft butt
Q_r	=	axial compressive load applied to the top of the drilled shaft rock socket
Q_{tip}	=	vertical load transfer, or tip resistance, at the drilled shaft tip
q_u	=	uniaxial compressive strength of rock core
w_c	=	displacement of the drilled shaft butt
w_{cr}	=	relative displacement between the shaft butt and the top of the rock socket
w_r	=	displacement of the shaft at the top of the rock socket
α_E	=	modulus reduction factor
ν_b	=	Poisson's ratio of rock mass below the drilled shaft tip
ν_c	=	Poisson's ratio of drilled shaft
ν_r	=	Poisson's ratio of rock mass above the drilled shaft tip
τ_{max}	=	average concrete-rock bound strength